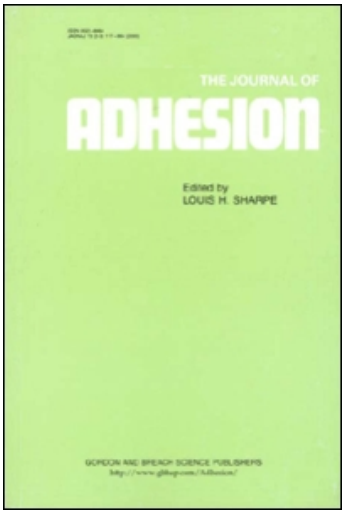

The Journal of Adhesion

Publication details, including instructions for authors and subscription information:
http://www.informaworld.com/smpp/title~content=t713453635

Interlaminar Stress Distribution Within an Adhesive Layer in the Nonlinear Range

S. Gal[a]; O. Ishai[a]
[a] Faculty of Mechanical Engineering, Technion-Israel Institute of Technology, Haifa, Israel

To cite this Article Gal, S. and Ishai, O.(1978) 'Interlaminar Stress Distribution Within an Adhesive Layer in the Nonlinear Range', The Journal of Adhesion, 9: 4, 253 — 266
To link to this Article: DOI: 10.1080/00218467808075119
URL: http://dx.doi.org/10.1080/00218467808075119

J. Adhesion, 1978, Vol. 9, pp. 253–266

Printed in Scotland

Interlaminar Stress Distribution Within an Adhesive Layer in the Nonlinear Range

S. GALI and O. ISHAI

Faculty of Mechanical Engineering, Technion-Israel Institute of Technology, Haifa, Israel 32000

(*Received November 28, 1977; in final form March 28, 1978*)

The solution for interlaminar stress distribution in an adhesive layer within a bonded structure is highly complex due to the predominantly inelastic nature of the polymeric adhesive. The present study attacks this problem using a nonlinear finite-element method and an empirical effective-stress–strain relationship derived experimentally for a typical epoxy adhesive loaded at a constant strain rate. The stress distribution in the critical zone of the interlaminar layer of a symmetric doubler model is presented.

INTRODUCTION

Numerous publications are available on analysis of the stress distribution within the interlaminar adhesive layer (IAL) of a structural bonded-joint model. Most of the earlier works[1-5] are based on certain assumptions (such as uniform shear and a normal stress distribution throughout the adhesive thickness) which facilitate a closed-form solution. These simplifications, however, yield only average stress data and make for certain inconsistencies in the equilibrium equations; some of them are incompatible with boundary conditions at the edges. More recent works try to get around the analytical complexity of the problem with the aid of numerical methods such as finite differences[6] and finite elements;[7-10] the latter, in particular, yield the two-dimensional stress distribution within the adhesive layer for models of isotropic[7,8] and orthotropic[5,9,10] adherends. These solutions are in agreement with the equilibrium and boundary conditions of the structural model but are confined to linear elastic cases.

By contrast, the polymeric adhesives commonly used in the interlaminar layer are characterized by nonlinear stress–strain behavior, even at relatively low stress levels. This behavior is even more pronounced at high stress levels, culminating in a plateau which may be termed "macro-plastic" yielding (see Figure 1). A simplified elasto-plastic model[10-12] may give an approximate upper bound to the real solution, but this is inadequate if we recall that under service conditions the material is not allowed to approach this level, while in the critical region of the adhesive, the stress is mainly in the nonlinear range.

The viscoelasto-plastic behavior of the adhesive, reflected in its sensitivity to time and temperature, also contributes to the complexity of the problem.

The present work, a preliminary attempt at a solution of stress distribution in a symmetric doubler model, is confined to the two-dimensional case and to constant temperature and strain rate (time) loading conditions.

CHARACTERIZATION OF THE ADHESIVE

Structural aluminum and a typical epoxy resin were selected as representative examples of a linear adherend and a nonlinear adhesive respectively. An effective–stress–strain relationship for the epoxy resin (Figures 1 and 2) was derived from the uniaxial stress–strain curves obtained by tensile and shear test data. The derivation is based on von Mises' deviatoric-energy yield

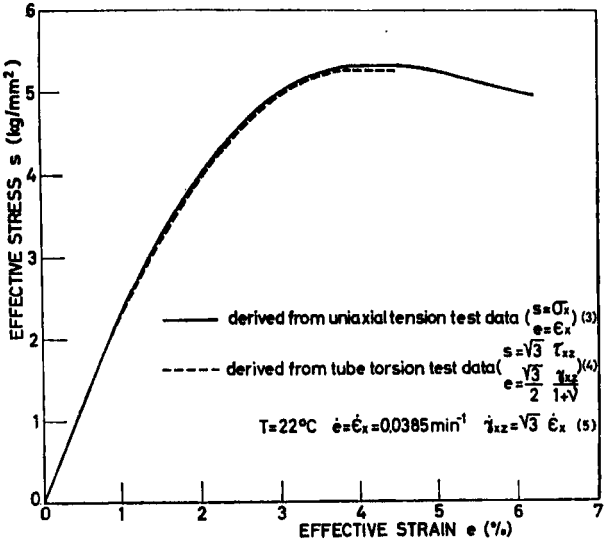

FIGURE 1 Effective–stress–strain relationship and related properties for epoxy resin used as adhesive layer.

criterion[13] in which S—the effective stress, and e—the effective strain, given for a general state of stress, are:

$$S = C_1[(\sigma_x-\sigma_y)^2+(\sigma_y-\sigma_z)^2+(\sigma_z-\sigma_x)^2+6(\tau_{xy}^2+\tau_{yz}^2+\tau_{zx}^2)]^{\frac{1}{2}} \quad (1)$$

$$e = C_2[(\varepsilon_x-\varepsilon_y)^2+(\varepsilon_y-\varepsilon_z)^2+(\varepsilon_z-\varepsilon_x)^2+6(\varepsilon_{xy}^2+\varepsilon_{yz}^2+\varepsilon_{zx}^2)]^{\frac{1}{2}} \quad (2)$$

where

$$C_1 = \frac{\sqrt{2}}{2}; \qquad C_2 = \frac{\sqrt{2}}{2(1+\nu)}; \qquad \varepsilon_{ij} = \frac{\gamma_{ij}}{2}.$$

The above formulations are reduced to Eqs. (3) and (4) in Figure 1 for the simple cases of uniaxial tensile and pure shear states of stress, respectively.

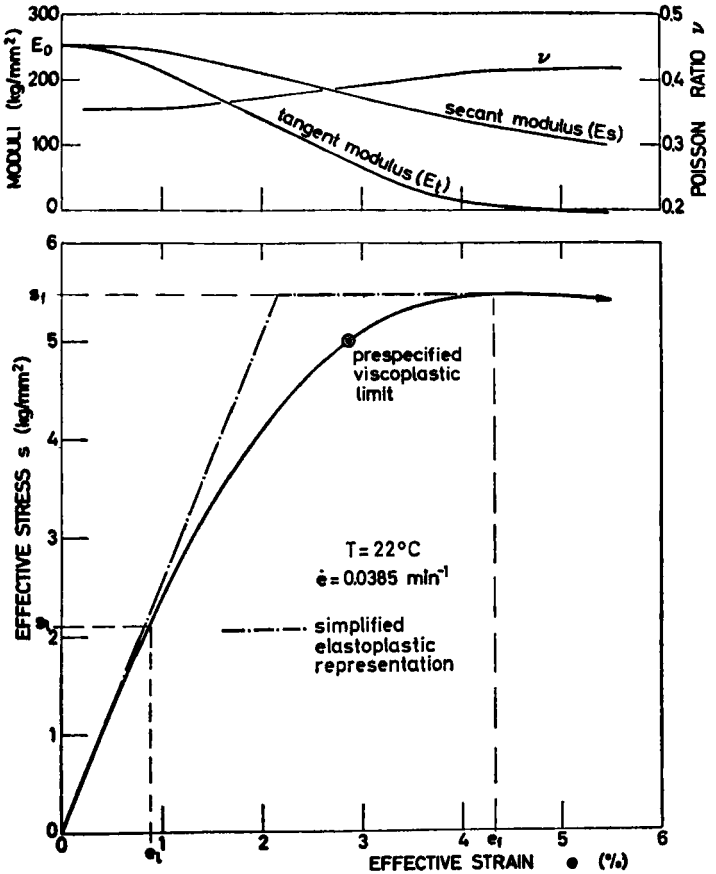

FIGURE 2 Effect of effective strain on variation of effective stress, Poisson's ratio and tangent and secant moduli of epoxy resin used for adhesive layer.

The effective tangent, E_t, and secant, E_s, moduli, and the effective Poisson ratio, ν, as well as the effective stress, S, are plotted against the effective strain, e, in Figure 2.

Three regions may be distinguished along the effective–stress–strain curve, namely:

1) An almost linear region up to the proportional limit, S_l, through which ν is almost constant.

2) A nonlinear (probably viscoelastic) region characterized by an increase in ν, up to the yield-plateau level, S_f.

3) A macro-plastic flow region beyond which stresses are almost constant and even tend to drop at higher strain levels; ν is again almost constant and its "inelastic" component tends to the value of 0.5 which is the theoretical limit for an incompressible-flow regime.

MODEL REPRESENTATION

IAL behavior is most conveniently illustrated by the symmetrical doubler (SMD) model shown in Figure 3 and described in Ref. 8, including the two-

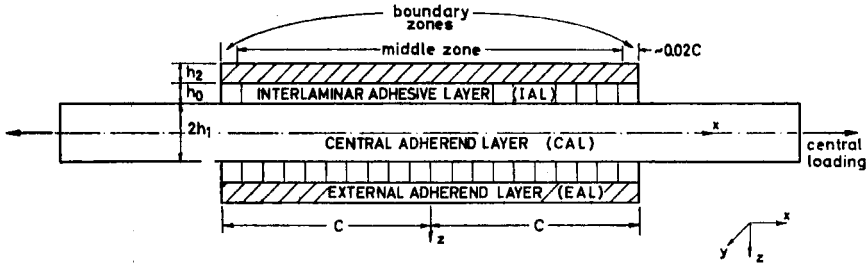

FIGURE 3 Symmetric doubler model.

dimensional linear elastic solution for the relevant stress distribution. The analysis focuses on the "boundary" edge zone where stresses attain their critical value; the corresponding finite-element network is shown in Figure 4.

ANALYTICAL PROCEDURE

The plane-stress and plane-strain states, which may be considered as bounds to the three-dimensional solution, represent the situation close to the free edges of the doubler width ($y = \pm b$) and along the midsection ($y = 0$)

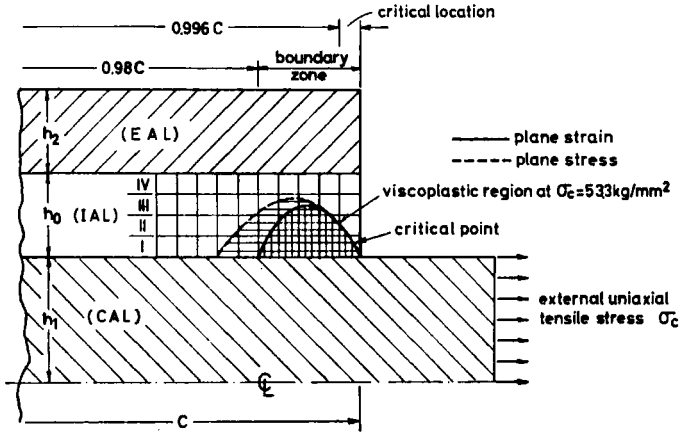

FIGURE 4 Illustration of IAL network at boundary zone used for finite element non-linear stress analysis.

respectively. The procedure for determining the stress distribution in the boundary zone under a given external uniaxial load follows the flow chart in Figure 5 and consists of the following steps:

1) Apply a predetermined external stress, σ_c, to the central layer.

2) Calculate the effective strains, e_k, and stresses S'_k, (Eqs. (1) and (2) respectively) for the different elements of the FE network, using the linear FE program described in Ref. 8 and assuming a uniform initial effective modulus, E_0, for all adhesive elements.

3) Determine the specific secant modulus, E^s_k, for each element (using the experimental relationship given in Figure 2), according to the corresponding effective strain, e_k, calculated in Step 2.

4) Rerun the program (steps 1 and 2) with the modulus for each element modified as per Step 3.

5) Compare the calculated stress, S'_k (Eq. (1)) for each element as derived in Step 4 with the "empirical" value S_k obtained from the effective–stress–strain curve.

6) Repeat Steps 3–5 until the difference between the calculated S'_k and "empirical" S_k stresses drops below 2% of the final stress value.

The procedure is illustrated in Figure 6 for a representative element k. Convergence, in the case of plane-strain, was achieved in a smaller number of iterations than on that of plane-stress (Figure 7).

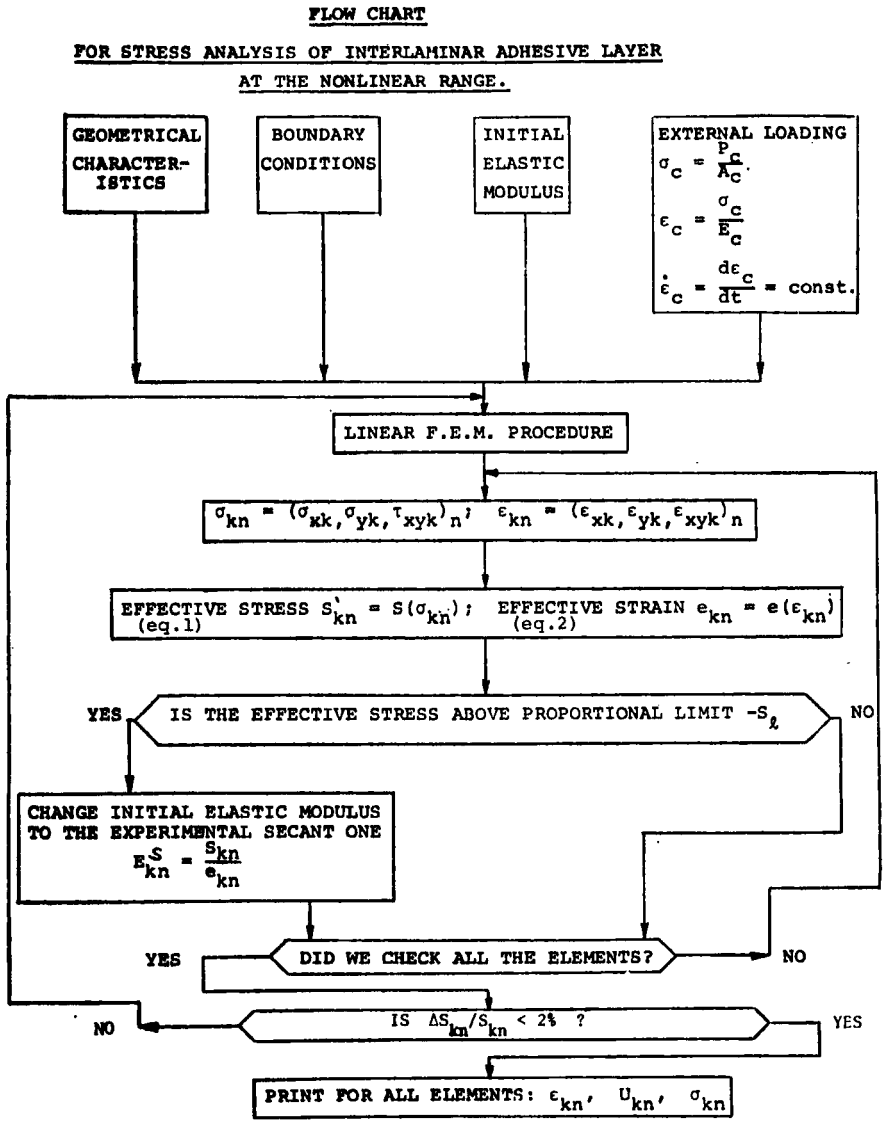

FIGURE 5 Flow chart for stress analysis of interlaminar adhesive layer in nonlinear range.

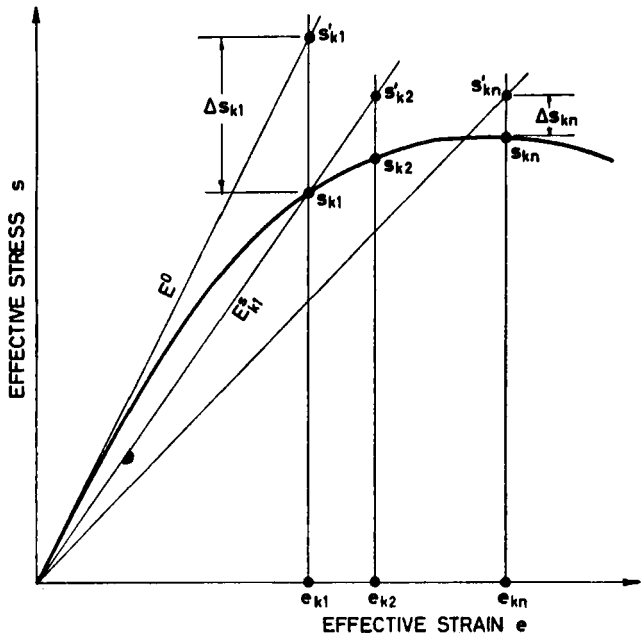

FIGURE 6 Illustration of FEM procedure for stress analysis of IAL in nonlinear range.

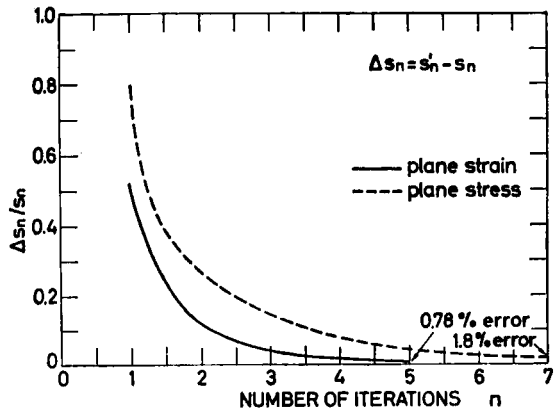

FIGURE 7 Convergence of FEM iteration procedure to exact solution.

STRESS DISTRIBUTIONS

The effect of external axial stress, σ_c, on the effective stress and strain at the critical point (close to the IAL edge; see Figure 4) is shown in Figures 8 and 9. The discrepancy between the linear and nonlinear solutions is pronounced, especially in the plane-stress case.

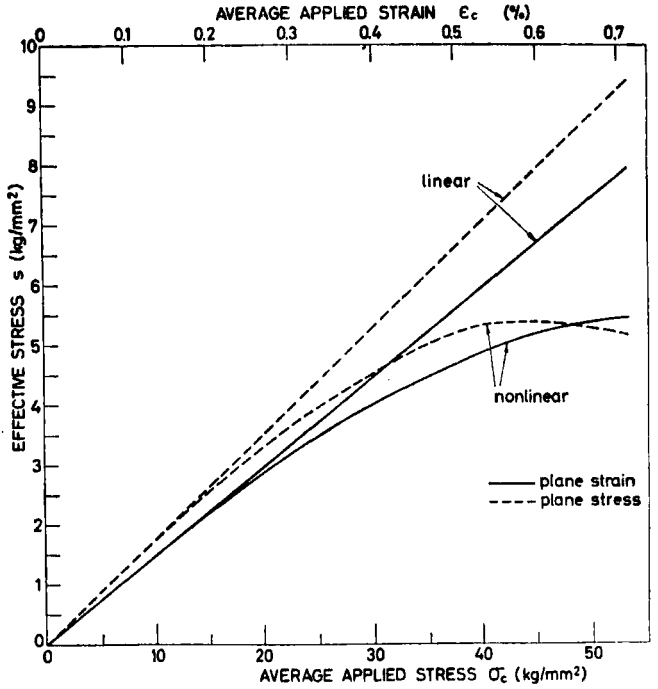

FIGURE 8 Effect of central loading on effective stress at critical point (see Figure 4) in boundary zone of IAL.

Lower effective stress and strain were found for plane-strain compared with plane-stress, while the opposite was the case regarding the shear (τ_{zxo}) and lateral normal (σ_{zo}) stress in the nonlinear solution (Figure 10); in the linear solution there was no significant difference.

The shear-stress distribution for $\sigma_c = 53.3$ kg/mm^2 is shown in Figure 11. Here again there is no significant difference between the plane states, except at the critical location (see Figure 4). Similar trends are seen for the lateral normal stress (Figure 12).

In most cases, the effective stress tends to level off and even drop faster in the plane-stress state.

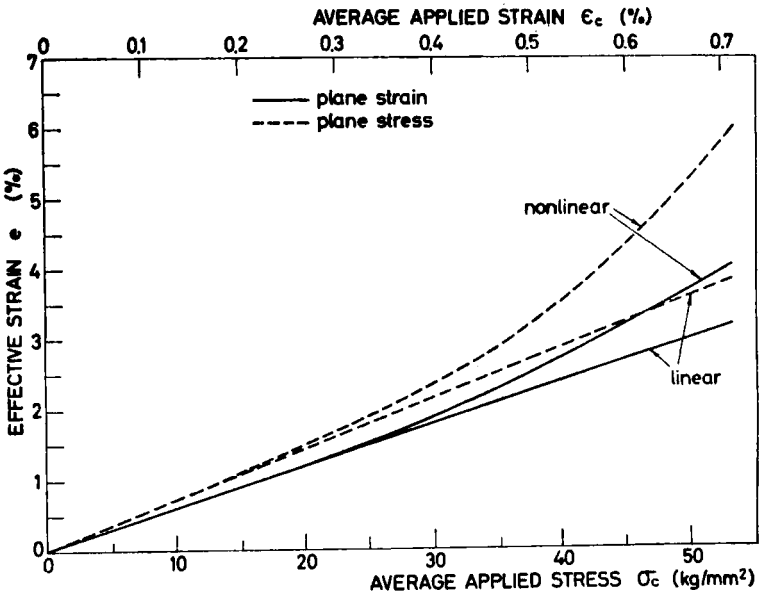

FIGURE 9 Effect of central loading on effective strain at critical point (see Figure 4) in boundary zone of IAL.

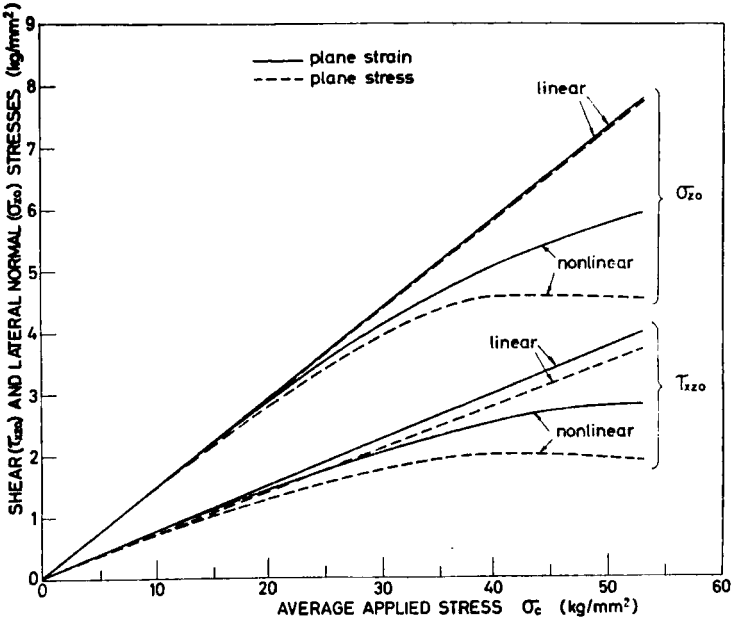

FIGURE 10 Effect of central loading on shear and normal stresses at critical point (see Figure 4) in boundary zone of IAL.

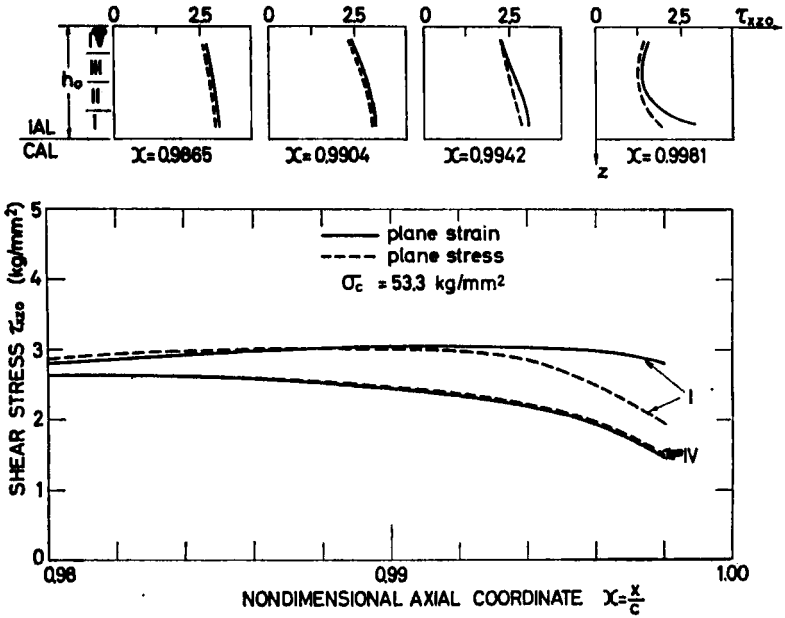

FIGURE 11 Shear stress distribution at boundary zone of IAL (nonlinear range).

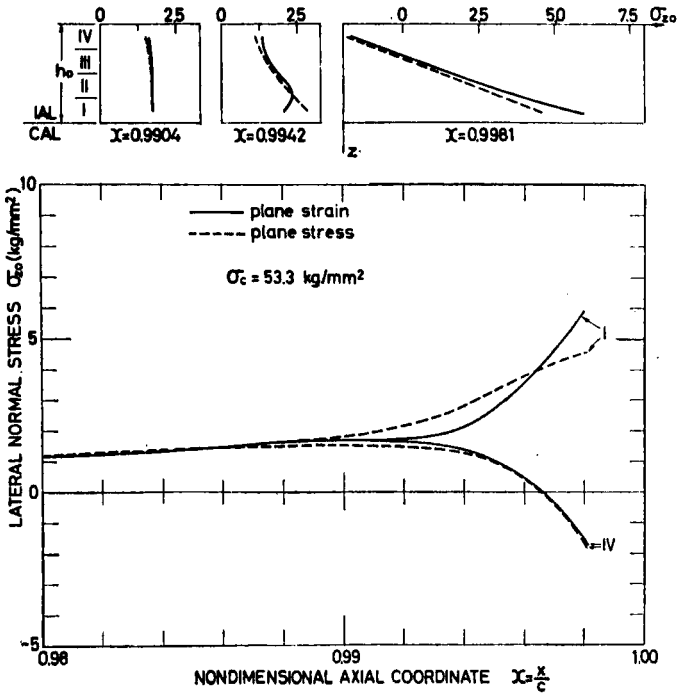

FIGURE 12 Lateral normal stress distribution at boundary zone of IAL (nonlinear range).

The effective-stress distribution at the boundary zone (Figure 13)† permits evaluation of the ductile failure process of the IAL. The region of "visco-plastic flow" includes the elements where the effective stress or strain exceed their prespecified limit,‡ as shown in Figure 2. For the specific load level of the present case, this region is located close to the lower edge of the IAL (Figure 4).

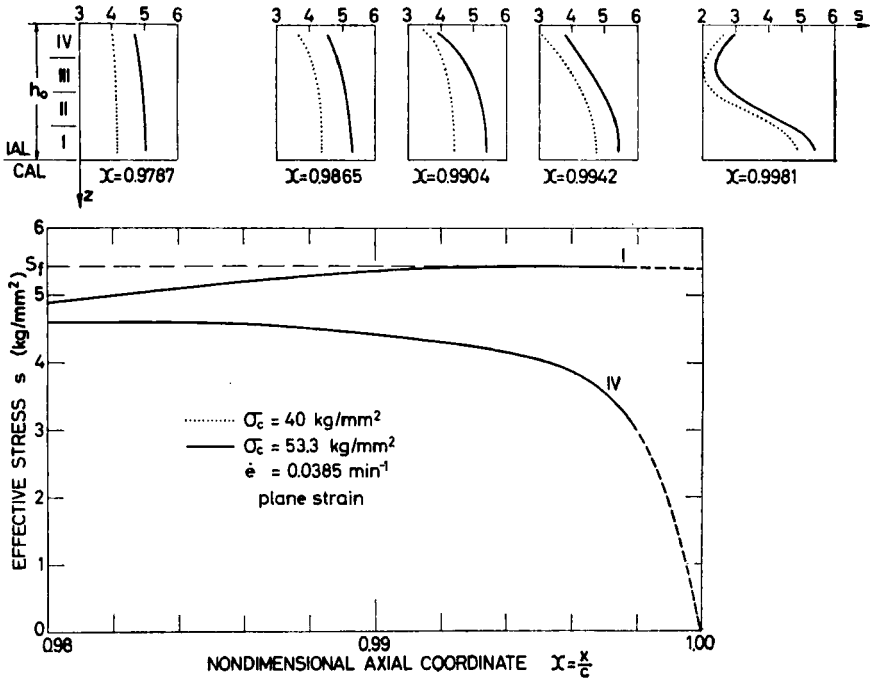

FIGURE 13 Effective stress distribution at boundary zone of IAL (nonlinear range).

COMPARISON WITH SIMPLIFIED ELASTO-PLASTIC SOLUTION

A simplified elasto-plastic model of the stress–strain relationship (Figure 2) has substantial advantages over the more realistic nonlinear one, in that it reduces the parameters for describing the complex inelastic process to two—the initial effective elastic modulus, E_0, and the effective-yield-stress plateau S_f. It also permits inclusion of the strain-rate and temperature-dependence

† The dashed lines are an extrapolation based on boundary conditions of zero stresses at the upper edge point (IV) and the upper bound of S_f at the lower edge point (I).

‡ This limit may be defined as the level where initiation of residual deformation was detected.

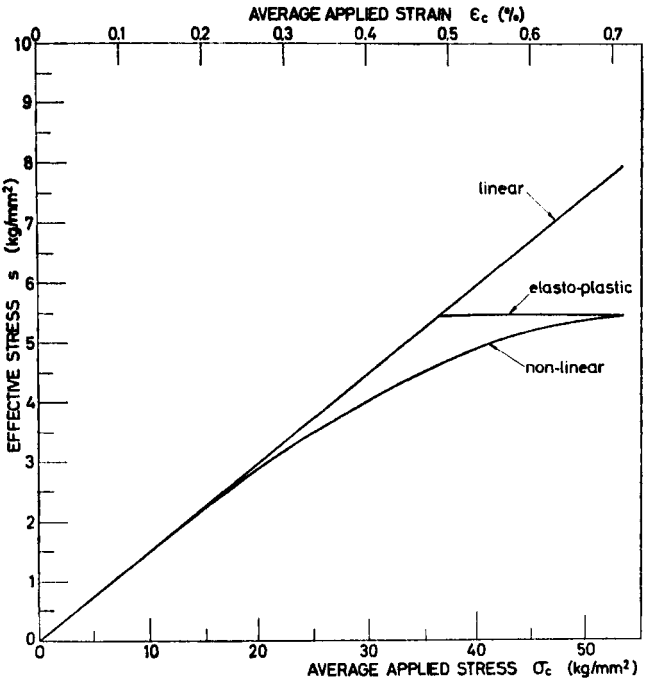

FIGURE 14 Effect of central loading of doubler on effective stresses at critical point in boundary zone of IAL (plane-strain, simplified elasto-plastic *vs.* inelastic solutions).

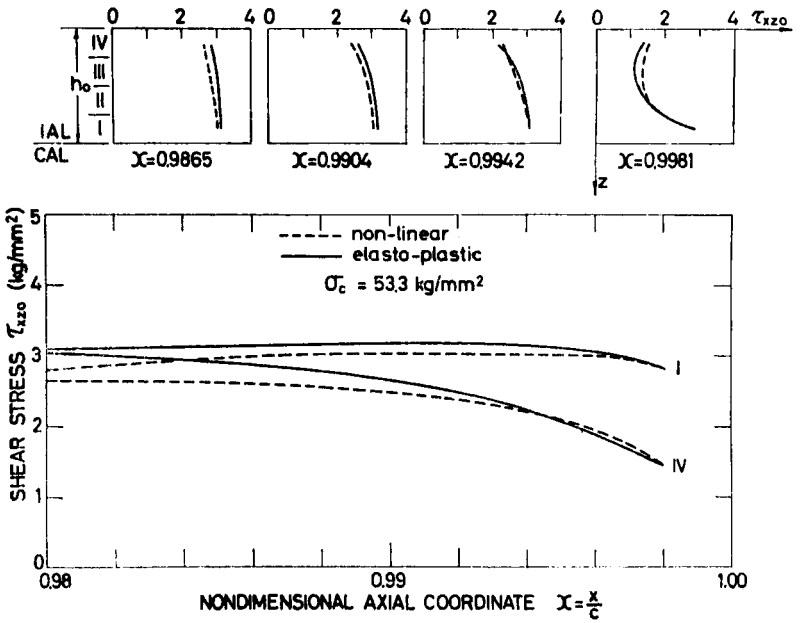

FIGURE 15 Shear stress distribution at boundary zone of IAL (plane-strain, simplified elasto-plastic *vs.* inelastic solutions).

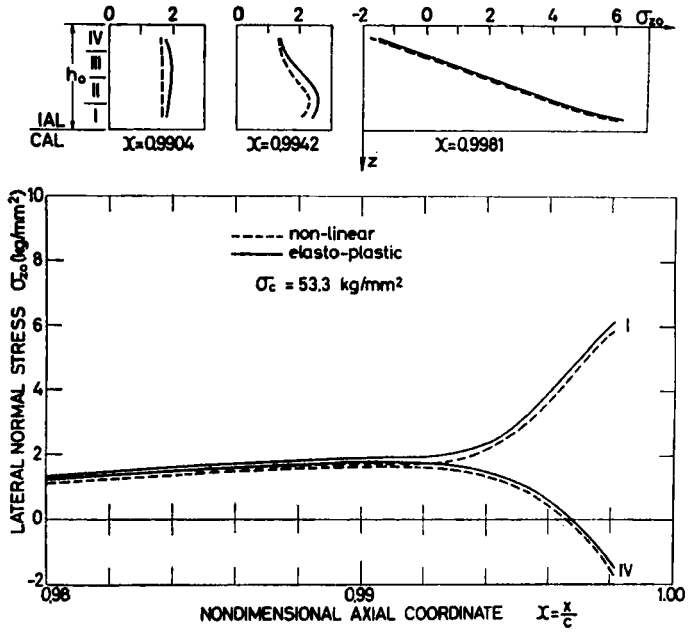

FIGURE 16 Lateral normal stress distribution at the boundary zone of IAL (plane-strain, simplified elasto-plastic *vs.* inelastic solutions).

in the analysis, provided their effect on the effective parameters are available[11,12,14]. The three stress distributions based on this model (Figures 14 to 16) show that while there is no significant deviation from the exact solution at the critical location (see Figure 4), there is some farther away from the edges.

CONCLUSIONS

1) A nonlinear FEM procedure was applied for determining the two-dimensional stress distribution within the interlaminar adhesive layer of a doubler model. The results can be used to predict a "visco-plastic" ductile failure mode within the adhesive, provided its effective inelastic stress–strain behavior and the corresponding failure envelope are available.

2) A significant difference in stress distribution was found between the linear and nonlinear solutions at the critical boundary zone close to the IAL edges. The assumption of plane-stress leads to a higher effective stress level and more conservative results where failure is concerned, compared with the plane-strain state.

3) A simplified elasto-plastic stress–strain relationship leads to a stress distribution similar to that obtained with the more realistic nonlinear stress-strain curve, in the critical zone.

4) The present study is a first step towards more general nonlinear numerical analysis of bonded structural systems. Future research will consist in time-dependent, nonlinear stress analysis of the IAL (with regard to the viscoelasto-plastic nature of the polymeric adhesive) and will also concern environmental effects (temperature, moisture) on the above time-dependent modes of behavior.

Acknowledgement

The present publication is based on the D.Sc. Thesis of S. Gali, to be submitted to the Senate of the Technion–Israel Institute of Technology. It is also part of a research project sponsored by the European Research Office, U.S. Army, under Grant Agreement No. DAERO–76–G–062.

References

1. M. Goland and E. Reissner, *J. Appl. Mechanics* **11,** A17 (1944).
2. R. W. Cornell, *J. Appl. Mechanics* **20,** 355 (1953).
3. E. W. Kuenzi and G. H. Stevens, "Determination of the Mechanical Properties of Adhesives for Use in the Design of Bonded Joints, US–FPL Report FPL–011 (1963).
4. O. Volkersen, *Construction Métallaine* **4,** 3 (1965).
5. W. J. Renton and J. R. Vinson, "The Analysis and Design of Composite Materials Bonded Joints under Static and Fatigue Loadings," AFOSR–TR–73–1627 (1973).
6. J. Pirvics, *J. Adhesion* **6,** 207 (1974).
7. R. S. Alwar and Y. R. Nagaraja, *J. Adhesion* **7,** 279 (1976).
8. O. Ishai and S. Gali, *J. Adhesion* **8,** 301 (1977).
9. D. Kutscha et al., "Feasibility of Joining Advanced Composite Flight Vehicle Structures." ITT Res. Inst. Technical Report AFML–TR–68–391 (1969).
10. J. N. Dickson, T. M. Hsu and M. J. McKinney, "Development of an Understanding of the Fatigue Phenomenal of Bonded and Bolted Joints in Advanced Filamentary Composite Materials," Vol. 1, Analysis Methods. Technical Report AFFDL–TR–72–64 (1972).
11. L. J. Hart-Smith, "Adhesive-Bonded Double-Lap Joints," NASA Contract Report No. NASA–CR–112235 (1973).
12. L. J. Hart-Smith, "Adhesive-Bonded Single-Lap Joints," NASA Contract Report No. NASA–CR–112236 (1973).
13. J. O. Smith and O. M. Sidebottom, *Inelastic Behavior of Load Carrying Members* (Wiley, N.Y., 1965), p. 86.
14. O. Ishai, *Polymer Eng. and Sci.* **9,** 131 (1969).